

# LOAN DOCUMENT

<p style="writing-mode: vertical-rl; transform: rotate(180deg);">DTIC ACCESSION NUMBER</p>	<p>LEVEL</p>	<p>PHOTOGRAPH THIS SHEET</p>	<p>INVENTORY</p>																		
<p><i>Fabrication of a Monolithic Single - . . .</i></p> <p>DOCUMENT IDENTIFICATION <i>Sep 96</i></p>																					
<p>DISTRIBUTION STATEMENT</p> <p>Approved for public release Distribution Unlimited</p>																					
<p>ACCESSION FOR</p> <table border="1" style="width: 100%;"> <tr> <td>NTIS</td> <td>GRAM</td> <td><input checked="" type="checkbox"/></td> </tr> <tr> <td>DTIC</td> <td>TRAC</td> <td><input type="checkbox"/></td> </tr> <tr> <td>UNANNOUNCED</td> <td></td> <td><input type="checkbox"/></td> </tr> <tr> <td>JUSTIFICATION</td> <td></td> <td></td> </tr> </table> <p>BY</p> <p>DISTRIBUTION/</p> <p>AVAILABILITY CODES</p> <table border="1" style="width: 100%;"> <tr> <td>DISTRIBUTION</td> <td colspan="2">AVAILABILITY AND/OR SPECIAL</td> </tr> <tr> <td style="height: 50px; vertical-align: middle;">A-1</td> <td></td> <td></td> </tr> </table>		NTIS	GRAM	<input checked="" type="checkbox"/>	DTIC	TRAC	<input type="checkbox"/>	UNANNOUNCED		<input type="checkbox"/>	JUSTIFICATION			DISTRIBUTION	AVAILABILITY AND/OR SPECIAL		A-1			<p>DISTRIBUTION STATEMENT</p> <p>DATE ACCESSIONED</p> <p>DATE RETURNED</p> <p>REGISTERED OR CERTIFIED NUMBER</p>	
NTIS	GRAM	<input checked="" type="checkbox"/>																			
DTIC	TRAC	<input type="checkbox"/>																			
UNANNOUNCED		<input type="checkbox"/>																			
JUSTIFICATION																					
DISTRIBUTION	AVAILABILITY AND/OR SPECIAL																				
A-1																					
<p>DISTRIBUTION STA</p> <p style="font-size: 2em;">19970114 022</p>		<p>DATE RECEIVED IN DTIC</p>																			
<p>PHOTOGRAPH THIS SHEET AND RETURN TO DTIC-FDAC</p>																					

HANDLE WITH CARE

UNCLASSIFIED

# FABRICATION OF A MONOLITHIC SINGLE-CRYSTAL SILICON INNER CONE SUBSTRATE FOR THE ROMA PROGRAM

Frank Groark

TRW, Inc.

One Space Park R1-1138  
Redondo Beach, CA 90278

## Abstract

Previous high energy laser mirrors were made of metals such as molybdenum, copper and tungsten carbide. These mirrors required active heat exchanger coolant systems to maintain the desired surface figure and were complicated and costly to manufacture. The successful use of uncooled, single crystal silicon mirrors for beam transfer optics in high energy lasers has demonstrated the feasibility of uncooled resonator mirrors. The Resonator Optics Material Assessment (ROMA) program surveyed the presently available technology for the fabrication of an uncooled inner cone optical element and then demonstrated the maturity of the technology by fabricating a single crystal silicon inner cone optical element for use in the Alpha space based high energy laser. The single crystal silicon inner cone is considerably simpler and can be manufactured using conventional machining techniques.

Key words: laser, resonator, inner cone, beam compactor, molybdenum, silicon, silicon carbide, Alpha.

## 1. Overview of the Beam Compactor Inner Cone

The inner cone optical element is the heart of the beam compactor, which is the main component in the Alpha space based high energy laser resonator (see Figure 1). The resonator annular leg is composed of a beam compactor and a rear cone. Turning flats and a scraper mirror provide the feedback leg. The beam compactor comprises an outer cone and an inner cone, each with two high energy optical surfaces. The purpose of the inner cone is two fold: the reflaxicon side takes the cylindrical beam reflected from the outer cone and compresses it into a solid cylinder (except for a small central hole caused by the truncated tip of the reflaxicon). The waxicon side of the inner cone takes the solid cylindrical feedback beam and expands it to the outer cone, which in turn creates a cylindrical beam that is amplified in the gain region. The inner cone is subject to high flux on the reflaxicon side and lower flux on the waxicon side,

and since it is a key element in the resonator, the optical distortion must be minimized.

The current Alpha inner cone is composed of copper clad molybdenum with three layers of spiral, counter-flowing heat exchangers under each of the optical surfaces. The heat exchangers are necessary to minimize distortion of the optical surfaces due to absorbed energy.

In contrast, a silicon inner cone with low absorption optical coatings does not need heat exchangers or coolant to maintain the optical surface figure. A low absorption coating coupled with the relatively high thermal conductivity of silicon makes a high power optic that maintains low distortion with no active coolant system. In addition, silicon has a low bulk absorption so that any energy that leaks through the coating is transmitted through the substrate. The uncooled single crystal inner cone substrate is 1/10th the cost and 1/4th the weight of the Alpha molybdenum inner cone, and takes 1/5th of the time to fabricate.

## 2. Comparison of a Molybdenum Inner Cone and a Silicon Inner Cone

### 2.1 Material

The current Alpha inner cone substrate is constructed of molybdenum. It has a three-piece substrate comprising a manifold plate and two optical surfaces. The manifold plate allows for the inlet and outlet of coolant and serves as a flow distributor for the optical surfaces. Each of the optical surfaces has a solid molybdenum powder metallurgy substrate that supports the heat exchangers. The heat exchangers are constructed of three vacuum arc cast (VAC) molybdenum plates that contain coolant channels and manifolds, and a top VAC molybdenum plate that forms the basis of the optical surface. The optical surface is electrodeposited Udylyte bright acid copper (UBAC), which is first diamond turned and then optically coated to form the final high energy surface. A sketch of the Alpha molybdenum inner cone is shown in Figure 2. Procuring the molybdenum

UNCLASSIFIED

required an international effort among several different European suppliers, because the material was not available domestically.

By contrast, the silicon inner cone was fabricated from one boule of single crystal silicon. The silicon was grown by the Czochralski method at Silicon Castings, Inc. The boule was approximately 16.5 inches in diameter and 17 inches long and weighed approximately 200 pounds. This is the largest known boule of single crystal silicon ever produced. The boule is shown in Figure 3 and the silicon inner cone is shown in Figure 4.

## 2.2 Coolant Requirements

The molybdenum Alpha inner cone requires approximately 125 gpm of water coolant, and the heat exchanger causes approximately 300 psi pressure drop. This requires large diameter plumbing and high pressure pumping capacity. In addition, the high velocity of the coolant water causes optics jitter and the large pressure drop induces distortion of the optical surfaces.

The single crystal silicon inner cone requires no cooling water and no plumbing or pumping system, thus significantly reducing total system weight and complexity.

## 2.3 Fabrication Time

Nominal fabrication time for the cooled molybdenum inner cone was 30 months and required a nation-wide network of subcontractors. The fabrication processes included: spin forming the heat exchanger plates, precision machining both the inside and outside contours of the heat exchanger plates, precision machining the substrate and related assembly components, brazing the heat exchanger plates to the substrate and the substrate subassemblies together, then precision machining the assembly. All of this was required to create the substrate; generation of the optical surfaces was yet to come.

To bring a single crystal silicon inner cone to the same point took approximately six months. The fabrication process consisted mainly of diamond grinding. The details of the fabrication process form the main content of this paper.

## 2.4 Weight

The molybdenum inner cone weighs 251 pounds, compared to 70 pounds for the silicon inner cone. This large reduction in weight is important for an on-

orbit device, but of even greater importance is the effect of removing the weight and volume of the water coolant and associated pumping, plumbing, and tankage systems. This also reduces the total system power requirements since no pump is needed, which reduces weight associated with batteries, solar arrays, etc. System complexity is further reduced since failure and abort points associated with the coolant system are removed.

## 2.5 Cost

Alpha actively cooled molybdenum inner cone cost was approximately ten times the single crystal inner cone fabrication cost. This cost comparison is for the substrate only, without the final optical surfaces and coatings. The cost reduction was due to a monolithic fabrication approach for the silicon inner cone, which eliminated operations for precision machining and assembly of separate piece parts.

## 3. Conical Test Article Fabrication

During the first phase of ROMA, several conical test articles (CTAs) were fabricated to investigate the geometry-dependent aspects of the fabrication process. The CTA is a prototype representing a chemical laser resonator inner cone optic, which fills the engineering gap between the two-inch diameter witness samples and a full-scale inner cone assembly. The Alpha waxicon inner cone was selected as the basis of design for the CTAs as it demonstrated many of the scaling issues within the size range of the available facilities (see Figure 5).

The CTAs were manufactured utilizing the same process(es) that would be employed for a real resonator optic. CTAs were fabricated from three materials: single-crystal silicon (SCSi), chemically vapor deposited (CVD) silicon carbide (SiC), and reaction-bonded (RB) SiC. The SiC material systems require a cladding to provide a diamond turnable surface for the ultimate figure and surface finish. The SCSi can be directly diamond turned. Of the three materials, single crystal silicon was found to be the best uncooled inner cone material because both the Czochralski process and the fabrication processes used to fabricate the CTAs were scaleable to the full inner cone size with no further development work and little risk.

### 3.1 Single Crystal Silicon

Fabrication of the single crystal CTAs was very straightforward, utilizing common fabrication processes and tooling. Four single-crystal silicon

boules were grown using the Czochralski process. The boules were diamond sawed and diamond ground to produce four eight-inch diameter by five-inch thick substrates, and then were diamond ground to the required shape. Two CTAs were chemically etched to remove the subsurface damage caused by the grinding operations.

### 3.2 CVD Silicon Carbide

CVD silicon carbide conical test articles were also investigated. The approach was to machine a female graphite mandrel and CVD 1/2 inch of silicon carbide. This approach, if successful, would reduce the amount of final diamond grinding of the optical surface because, when separated from the mandrel, the replicated CVD silicon carbide would be near-net-shape and the center would be hollow.

However, all of the attempts to manufacture a CVD SiC CTA were unsuccessful because the CVD SiC process was not compatible with the existing waxicon CTA shape. The tip area of the graphite mandrel caused a stagnation of the CVD gases, creating carbon rich area near the tip that had a very low deposition rate. The reference surfaces around the perimeter of the CTA also exhibited abnormal build up, with excess material on the outside corners and minimal material in the inside corners. Also, the release agent deposited on the graphite did not work well near the sharp edges and allowed the deposited SiC to impregnate the graphite mandrel at these edges. All of the CVD CTAs cracked when they were cooled to room temperature. This was due to the coefficient of thermal expansion (CTE) mismatch between the graphite mandrel and the CVD SiC CTA. The CVD SiC process was dropped from further ROMA consideration because the process requires further development and has a long processing schedule, a very high projected cost, and very high fabrication risk.

### 3.3 Reaction-Bonded Silicon Carbide

The RB SiC process consists of casting and sintering a SiC form. This is followed by infiltrating the porous SiC body with silicon. Four CTAs were ultimately produced from 14 initial castings. These four were ground to contour and two were clad with PVD silicon. The RB SiC CTAs were hollow, similar to the CVD CTA design.

A phase change from liquid to solid during the cooling portion of the siliconization process caused

an 8% expansion difference between the silicon and the silicon carbide, which caused ten of the 14 CTAs to crack. It is possible that this cracking problem could be controlled by maintaining uniform temperatures and a very slow cooling rate; however, such a study was not included within the scope of this project. Development work is required to improve the yield of the siliconization process. The PVD silicon cladding process (to allow single point diamond turning of the optical surface) also needs further development to reduce defects that would ultimately compromise the optical surface.

## 4. Inner Cone Assembly Fabrication

Based on the results of the conical test article work discussed in Section 3, single-crystal silicon was chosen for scale up to the full-size inner cone.

### 4.1 Inner Cone Assembly Design

Two approaches were investigated for fabrication of an uncooled inner cone substrate. The first was to fabricate the inner cone in two or three separate pieces as shown in Figure 6.

This approach would require more processing steps than the monolithic inner cone approach. Each piece must be machined to near net shape, each individual piece must be etched to remove the machining surface damage layer, and the surface to be brazed must be then precision match-machined to maintain approximately a 0.001 inch gap over the brazed area. To maintain assembly concentricity, each part must be machined to allow installation of an alignment pin. Braze tooling must be designed and fabricated to maintain contact pressure and inner cone assembly alignment to assure 100% braze of the three pieces. After brazing, the entire inner cone assembly must be re-diamond ground and chemically etched prior to brazing the mounting inserts and brazing on the tangent mount assembly. Because of the relative complexity of the fabrication process, this multi-piece approach was not selected.

The second approach was to fabricate a monolithic silicon ingot from which the inner cone shape could be generated. This approach was selected for further study. Although the monolithic silicon material was considerably more costly than the material for the segmented approach, that cost was more than offset by savings in reduced fabrication time and the reduced risk of the monolithic approach.

#### 4.2 Inner Cone Substrate Ingot Fabrication

Fabrication logic for the monolithic silicon ingot approach is summarized in Figure 7. The additional cost of the monolithic silicon ingot more than offset the fabrication time, risk, and cost to bond together a segmented inner cone substrate. Silicon Casting, Inc. has a very large single crystal Czochralski station and can pull a single crystal silicon ingot up to 275 lbs. The inner cone substrate requires a typical cylinder 13 inches diameter by 15 inches in length plus material for machining and chemical etching tolerances.

The fabricated ingot, which weighed 200 lbs, is shown in Figure 3. It was 17 inches high by 16.5 inches diameter, with a taper at the neck. The boule was near-net-shape to the reflaxicon end of the inner cone assembly.

#### 4.3 Inner Cone Substrate Ingot Rough Shape Diamond Grinding

The boule was mapped to determine the location of the inner cone rough shape as shown in Figure 8. The inner cone shape was generated in two stages of diamond grinding: First, a milling machine was used to rough grind the ingot to the rough shape dimensions. Then, following an etch process to remove subsurface machining damage, the substrate was precision machined on a computer-controlled mill to its final shape.

The rough machining operations were performed by LTD Ceramics on a conventional, manual, Bridgeport milling machine modified for the tall height of the boule. Two spacers were added to raise the mill head 14 inches to provide clearance for the silicon boule resting on a tilt fixture and rotary table. The rotary table was bolted to the bed of the machine, providing a fourth axis to produce the surfaces of revolution of the inner cone. A multi-axis tilt fixture was designed to hold the ingot and be mounted on the rotary table. This fixture allowed angular and spatial positioning of the inner cone boule for initial rough machining.

The reflaxicon side of the inner cone boule had to be ground in three stages down the surface of the cone because the mill's maximum travel was only 7 inches. The milling head was rotated 42.5 degrees and the surface was machined by starting from the tip and moving to the outside diameter. Approximately 3/8 inch of material was removed to create the reflaxicon surface.

The milling head was rotated back to the vertical position and the outside diameter of the inner cone was then machined from the original 16.5 inches diameter to 13.31 inch diameter. The diameter was finished about 3 inches down the boule to allow mounting of an aluminum tangent mount cylinder. The mount cylinder allows the inner cone to be safely handled and mounted to machining fixtures. The previously described tilt fixture was removed from the rotary table and replaced with a fixture to interface with the tangent mount. This fixture allows access to finish the outside diameter and rough machine the waxicon side.

The waxicon side of the inner cone boule was rough ground in two steps: First, the diameter was reduced from the 16.5 inches to 8.0 inches. Then, the milling head was rotated 39 degrees and the waxicon straight contour was ground.

#### 4.4 Inner Cone Substrate Chemical Etching

Following rough grinding, the inner cone was chemically milled to remove material off all surfaces of the substrate. This process was developed by TRW for chemical milling of conventional silicon turning flat optics. The milling action is monitored by periodically removing the cone and performing dimensional measurements to calculate the milling rate.

After chemical milling, the inner cone was inspected on a coordinate measuring machine (CMM) to determine the starting dimensions for precision machining. The inspections identified an interesting phenomenon: the preferential etching of the (100) and (110) planes. The waxicon and reflaxicon optical surfaces had a 4 lobe azimuthal profile variation that corresponded to the fast-etching (100) plane of the crystal. The peak-to-valley variation was on the order of 0.020 inch after both chemical milling steps were complete. In comparison, the substrate OD section showed a 4 lobe variation of only 0.009 inch. This preferential etching is due to the anisotropic etching processes. The slowest etching planes are those that are close packed; in silicon, these belong to the (111) family. The fastest etching planes have the most open structure. The atoms of the (100) family of planes are most widely spaced in silicon. The (110) family of planes have an intermediate etch rate.



To visualize the anisotropic etching of the optical surface, Figure 9 shows that the inner cone may be viewed as layers of the (100) planes stacked one upon another, with each circular plane becoming progressively smaller in area as the tip of the cone is approached. After etching, the four-lobed clover leaf pattern appeared, with the lobes corresponding to the crystal growth corners. This result is expected because the corners of the crystal comprise intersection (110) planes, which have a slower etch rate than the (100) planes that make up the faces of the cubic structure. So the high points on the lobes are the 4 crystal corners made up of (110) planes. The valleys between each of the lobes correspond to the (100) faces. These faces can be traced all the way to the tip of the cone, which was etched to a nearly perfect square.

Figure 10 depicts the anisotropic etching of the cubic crystal contained within a cylinder. The (100) planes, which comprise the faces of the cube, are only exposed at the top and base of the cylinder. The other four faces are buried within the cylinder. The four edges of the cube, which intersect the surface of the cylinder, are the (110) planes which define the growth nodes. The material between the buried faces and the cylinder surface are comprised of (111) planes. Since the 111 family of planes are the slowest etching, and the only other exposed material corresponds to the (110) planes (which have a faster etch rate), then the growth nodes should be expected to be the fastest etching region.

#### 4.5 Inner Cone Substrate Precision Machining

Following the chemical etching process, the inner cone substrate was transported to Raychem for precision machining on a Mori Seiki computer controlled milling machine. A precision rotary table was installed on the bed and integrated with the computer control.

A program based on the optical surface contour polynomial was written to control the machine to precisely generate the optical contours and reference surfaces. The program included a user interface that allowed the machinist to input grinding wheel diameter and tool edge radius. These tool features must be accurately defined to allow the program to accurately calculate the tool contact point and the associated tool path. As can be seen in Figure 11, the contact point of the tool changes as a function of the slope of the conical optical surface. The tool path, in the machine's coordinate system, was defined by the

path of the point defined by the tool's center line and bottom edge. The origin for the parts coordinate system, which defined the cone's optical contour, was at the theoretical tip of the cone. The coordinate system of the cone had to be transferred to the machine coordinate system based on the profile features of the grinding wheel. The program was written to allow the operator to input the values of the specific grinding wheel that was being used. The program then calculated the machine tool path to cut the optical contour based on cutting tool features. The tool path from the program was then loaded into the machine controller and the tool path was executed.

During initial inner cone set-up and coordinate system definition, it was discovered that the grinding wheel was not a precise shape. The wheel had run-out in diameter, edge radius, and flatness on the bottom of the tool. The run-out was caused by errors in the tool, not errors in the machine spindle. The same qualities of the metal matrix diamond wheel that reduce the tool wear also make it very difficult to cut the wheel to a desired shape. This potential problem was overcome by performing a cutting test. The test allowed the tool's effective diameter and edge radius to be determined by cutting a sample, then inspecting its shape and determining the effective features of the tool. The effective dimensions of the tool were then input into the program. This process allowed the use of standard quality grinding tools and saved the cost and schedule that would have been associated with creating a precision grinding wheel.

The machining plan for the inner cone included extra stock on top of the inner cone final dimensions for such things as chemical milling prior to single point diamond turning (SPDT), stock for SPDT, and stock for future rework. The stock was added to the inner cone by axially displacing the waxicon and reflexicon contours. This allowed the actual optical contours to be used in the precision machining process. If the stock had been added normal to the surface, as is often the practice in machining, a new contour equation would be required for nearly every cut, making traceability to the optical contour difficult. Radial stock was added to the reference surfaces at the same time; however, this had no effect on the optical contour profiles.

The first activity at Raychem was to grind the outside diameter down to 13.100 inches and install the final aluminum tangent mount cylinder. The tangent flange had been removed to allow chemical milling of the inner cone. A fixture was installed that supported the

inner cone on the waxicon substrate side and allowed precision machining of the outside diameter of the substrate. Without breaking the set-up, the new tangent flange was installed and positioned with a dial indicator. The flange was then inspected and deemed not flat enough for its planned use as a machining datum, so the flange was precision machined while bolted to the substrate. Both the top and bottom surfaces of the flange were machined to achieve 0.0002 inch flatness and parallelism. The outside diameter was machined round to 0.0002 inch total indicated reading (TIR).

The same fixture that was used during rough machining on the Bridgeport was then mounted on the Mori Seiki and nominally centered. The fixture mounting surface was machined flat to 0.0002 inch. The inner cone was then mounted with the reflaxicon surface facing up. The flatness of the tangent flange on the substrate was checked and used as a guide and the mounting bolts were tightened. The substrate outer diameter was used to center the assembly to 0.0002 inch and the flatness was rechecked.

The reflaxicon side was precision machined first. Since the rough machined cone was a linear cone, the optical contour was rough machined first. After the contour was rough machined, the reference surfaces were added and then the final finish cuts were made on the optical surface. Initially, an X axis feed rate of .100 inch per revolution was used to rough in the contour. Then, progressively finer feed rates were used until the final contour tolerances and surface finish were reached.

The identical process was used to machine the waxicon side.

#### 4.6 Machining Parameters

To produce good surface finishes with the metal matrix tools, very fine feed rates and shallow depths of cut must be employed and fine grit wheels must be used. The values selected for depth of cut, feed rate, surface speed, spindle rpm, part rpm and cutting fluid all affect part accuracy and surface finish. Also, tool type (radius edge tools or straight edge tools), length of tool shaft, and starting and finishing on sharp edges or corners all affect the choices made for the cutting parameters. Finally, cutting direction has a significant impact on the final product.

For machining the inner cone, computer control was used extensively to maintain optimum cutting parameters throughout the tool path.

The depth of cut was varied depending on the amount of stock on a surface. The stock was removed in a series of machining steps with continuously reduced depths of cut until only approximately .005 inch of stock remained. At that point the finish cuts were planned so that one semi-finish cut and one last finish cut were required. At this point, great care must be taken to ensure that the final dimension and surface finish is within tolerance.

The tool feed rate, as shown in Figure 12, was in the x-axis. Feed rate is one of the most important machining parameters, as it has a direct effect on the surface finish and is directly controlled by the machinist through the computer controlled machining program. The feed rate also directly affects the height of the cusp of the tool. It is desirable that the feed rate be as slow as possible for the best surface finish; however, slow feed rates make for very long cutting sessions and reduce productivity. The feed rate must then be coordinated with the roughing cuts, depth of cut, and surface speed such that acceptable surfaces are generated in the minimum amount of time. The cutting plan must continually improve the surface finish so that, as the final cuts are approached, the surface is very near final contour and roughness. The final cut has the slowest feed rate and shallowest depth of cut.

#### 4.7 Diamond Grinding Wheel Design

The diamond grinding wheels fall into two categories for silicon machining. A metal matrix diamond wheel is used on large surface areas that are free of small detail features. A resin bonded diamond wheel is used for small detailed work in areas such as the inner cone reference surfaces.

In general, the best surface finish was achieved with the resin bonded wheel but at the price of greater tool wear. Actual tool wear was not quantified during inner cone machining; instead, the tool was used to cut within a few thousandths of an inch of the final surface and then was dressed before the final cut to size. The final pass did not remove extensive material, so there was very little tool wear and no correction was required. The resin bonded wheels cut freely because the resin bonding material continually wore, exposing new, sharp diamond crystals.

In contrast, metal matrix wheels have no significant tool wear when cutting silicon but do not produce fine surface finishes as easily as the resin bonded wheels. This is because the metal matrix holds the diamonds very firmly. During the machining process,

the sharp edges of the diamonds are dulled and the cutting quality is reduced. To improve the cutting action, the wheel must be periodically dressed with a silicon carbide wheel. The dressing operation chips the dull diamonds and exposes new sharp edges. When the silicon inner cone was machined, this dressing operation was accomplished without significantly altering the tool dimension, so no recalibration of the effective cutting parameters was required. To produce good surface finishes with the metal matrix tools, very slow feed rates and shallow depths of cut must be employed, along with fine grit wheels.

Each diamond wheel contains 72 carats of diamond. The metal matrix is an alloy designed to effectively bond the diamonds. Diamonds are mixed throughout the approximately 1/8 inch thick diamond edge (see Figure 13). The diamond tool roughness (grit size) and condition (sharp or dull) have a significant influence on surface roughness and uniformity. To generate the most uniform surface finish, the tool was redressed one cut prior to the finish cut. The first cut after redressing often showed variable surface finish. This may have been caused by a rapid breakdown of the newly sharpened diamond edges. The surface finish became smoother and more uniform after several minutes of machining with the newly sharpened tool. The surface finish quality could then be maintained for many shallow finish cuts or several deep roughing cuts.

To maintain high quality surface finishes the machinist must be observant and listen to the characteristic sound that a freely cutting wheel makes and visually inspect the machined surfaces. If the wheel is vibrating and making odd noises, the machinist must inspect and redress the wheel; otherwise, both dimensional tolerances and surface finish will be negatively affected. Further

investigation and experience may lead to more quantitative measurements of the grinding wheel's condition, but the results achieved on the inner cone indicate that close observation of the tool's cutting characteristics can lead to very good results.

### Conclusion

With the completion of precision grinding the inner cone is ready for diamond turning of the high power optical surfaces and alignment reference surfaces. Diamond turning of the inner cone will be addressed in a future paper.

### Acknowledgements

The Resonator Optics Materials Assessment (ROMA) program was performed on the TRW Space and Defense, Zenith Star contract number GH8-180564 to Lockheed Martin Astronautics under their Zenith Star prime contract number SDIO-89-C-0003 to the Ballistic Missile Defense Office (BMDO).

The author would like to thank Dr. Lyn Skolnik of the Ballistic Missile Defense Office and Mr. Larry Buelow of Lockheed Martin Astronautics for sponsorship, and Dr. Larry Zajac, Dr. Bob Field, Dr. Phil Goede, Dr. Bill Goodman, Mr. Bruce Heckert, Mr. Chris Lieto of W. J. Schafer Associates, Inc., and Dr. Gary Morr of SAIC for their technical assistance. Thanks also go to Dr. Jim Boyle of Silicon Casting Inc. in Rancho Cordova, CA, Mr. Doug McCarter of McCarter Machine Co., Inc. in Pasadena, TX, Mr. Robert Fairbanks of Scarrott Metallurgical Services in Los Angeles, CA, Mr. Matt Chmait of TRW in Redondo Beach, CA, and Mr. Jim Hamilton, Mr. Steve Bretz, and Mr. Charlie Giles of Lawrence Livermore National Laboratory in Livermore, CA for technical contributions.



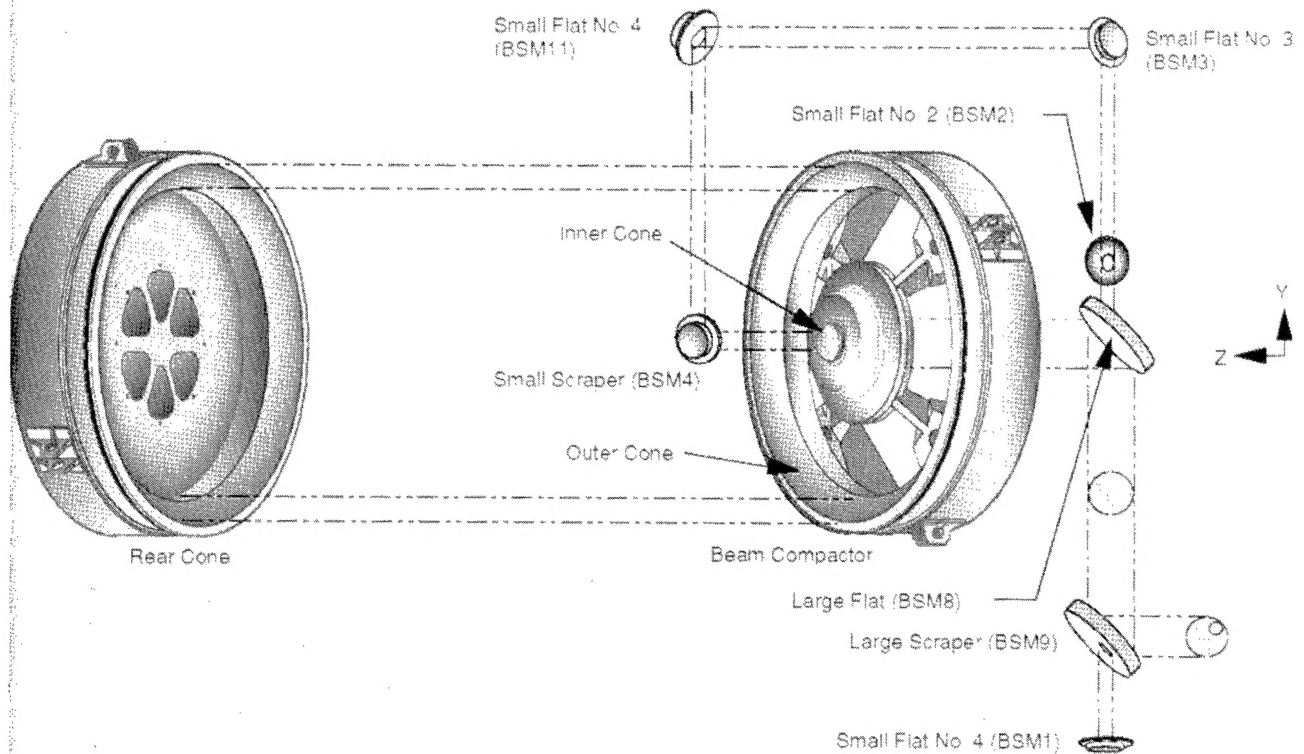


Figure 1. Alpha Laser Optical Resonator Assembly

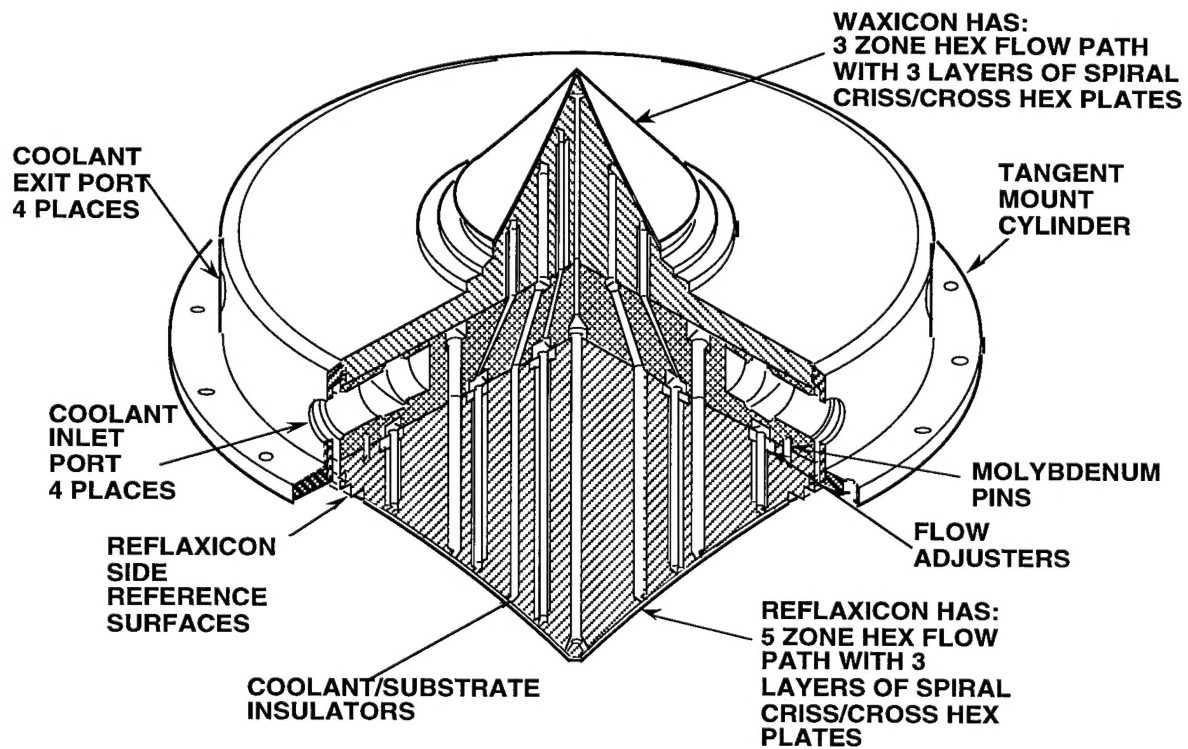
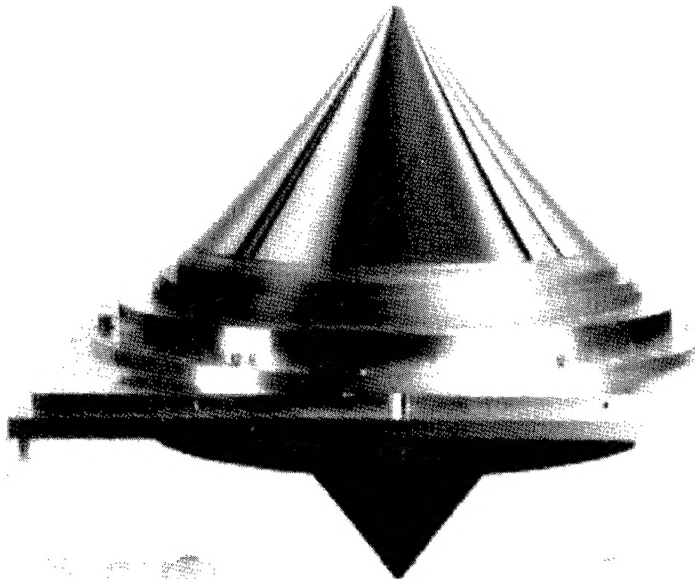


Figure 2. Alpha Molybdenum Inner Cone

UNCLASSIFIED



**Figure 3. Single-Crystal Silicon Boule Fabricated for the Monolithic Inner Cone**



**Figure 4. Monolithic Uncooled Single-Crystal Silicon Inner Cone**

UNCLASSIFIED

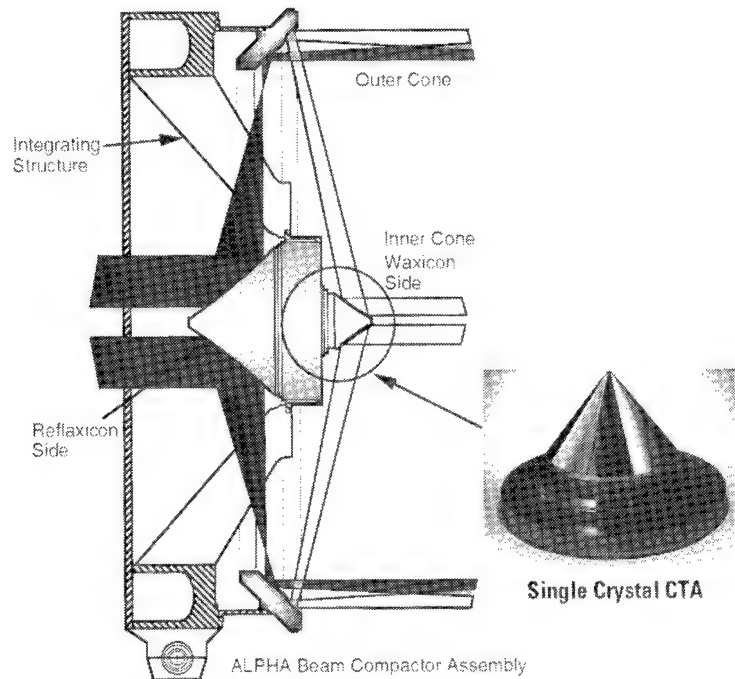


**Figure 5. Conical Test Article Based on Alpha Waxicon Inner Cone**

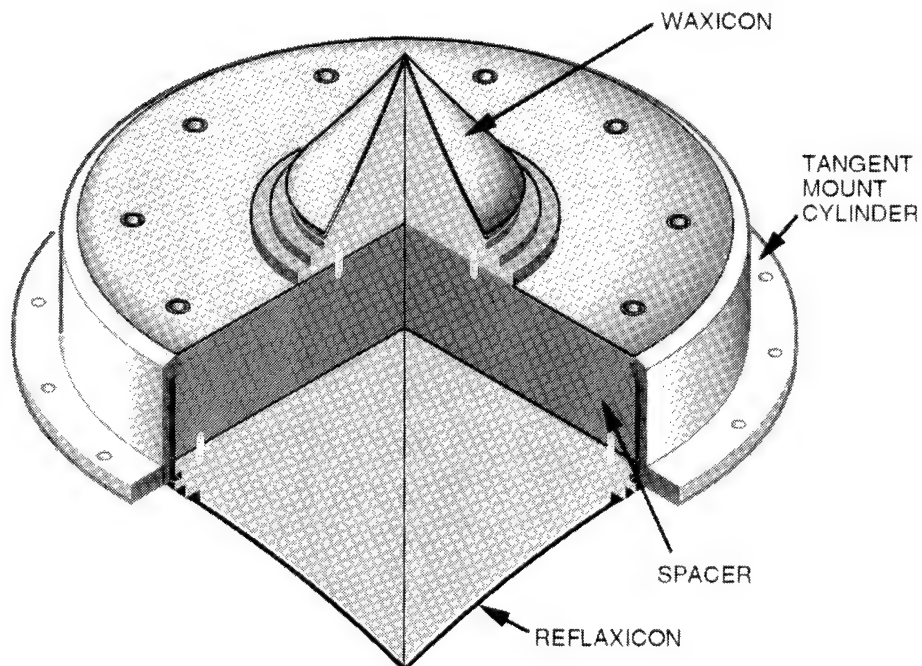


**Figure 6. Multi-piece Uncooled Inner Cone Concept**

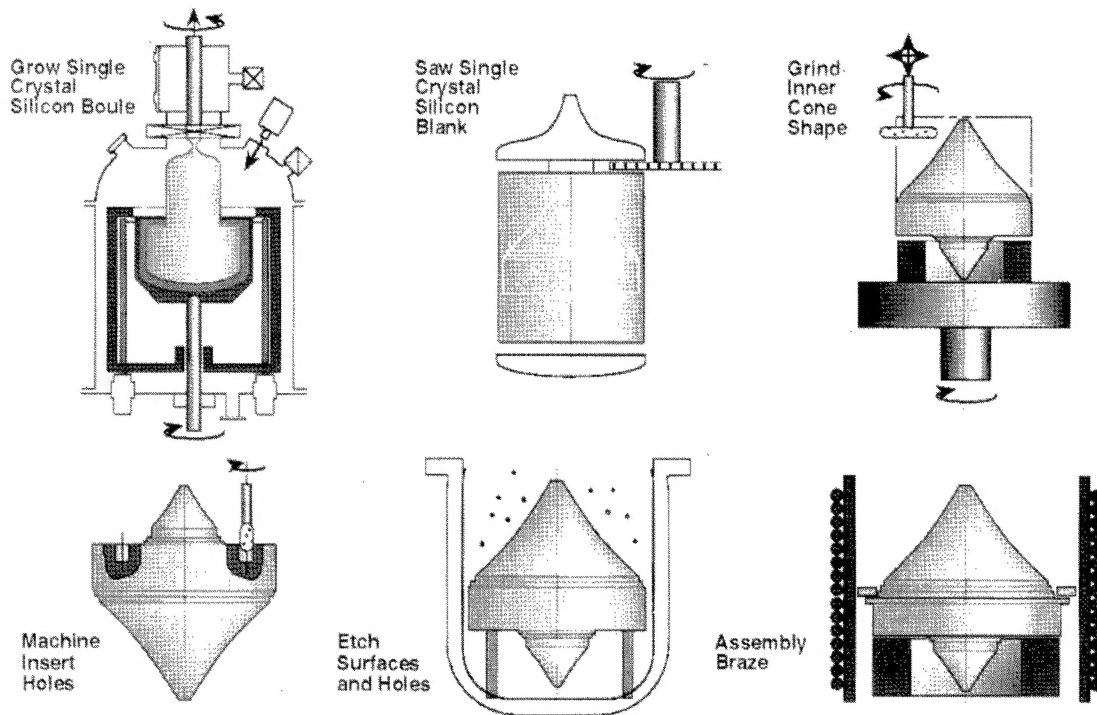


Figure 7. SCSi Inner Cone Fabrication Logic

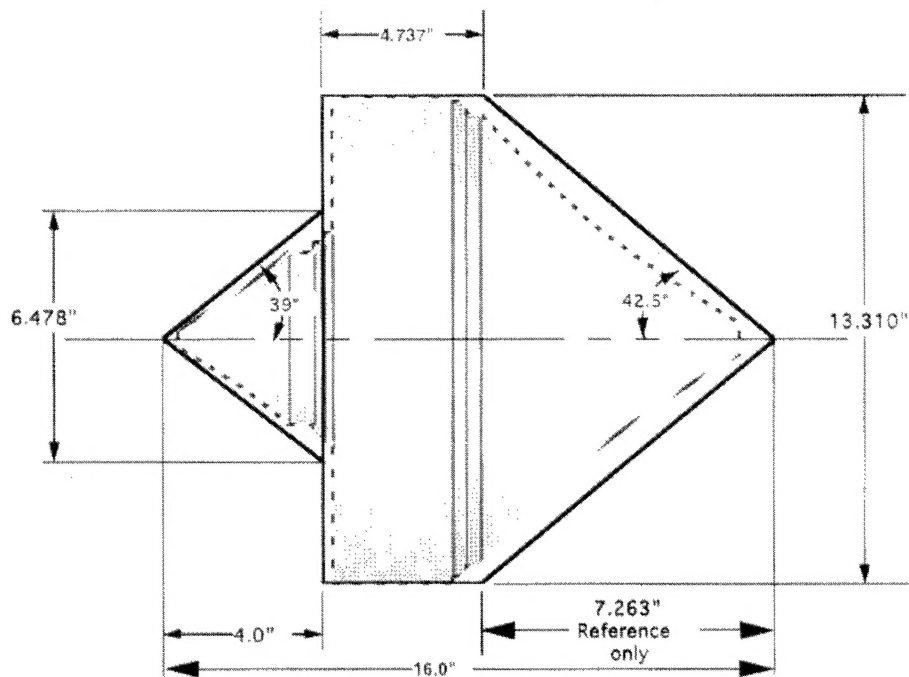
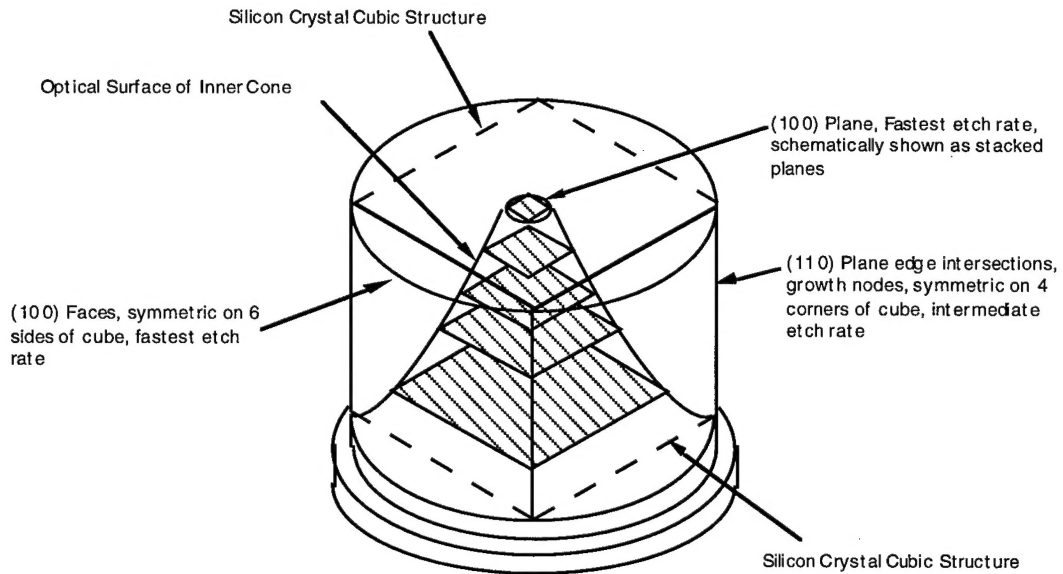
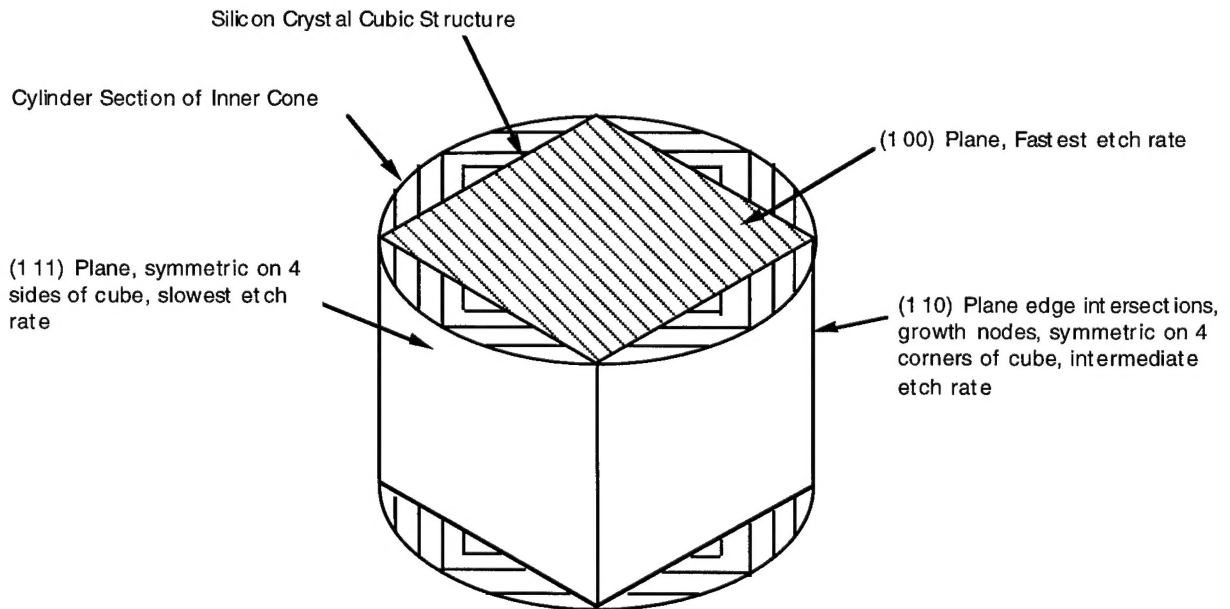


Figure 8. Inner Cone Shape to Rough Machined Boule

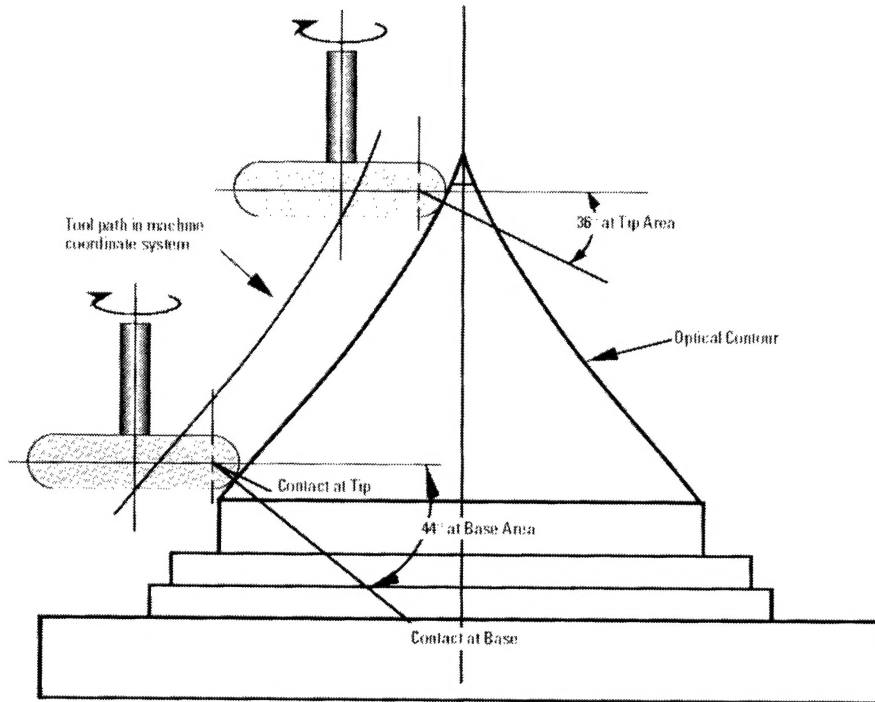


**Figure 9. Relationship Between Crystal Plane Etch Rate and Inner Cone Optical Contour**



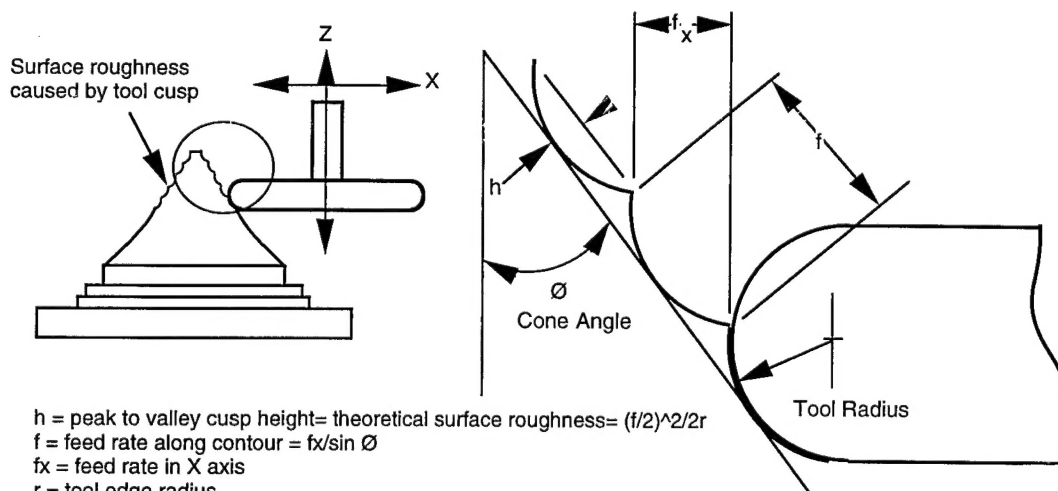
**Figure 10. Relationship Between Crystal Plane Etch Rate and Inner Cone Cylinder Section**





Contact point of tool and optical contour change as function of axial position

Figure 11. Tool Path and Contact Point of Tool Edge



$h$  = peak to valley cusp height = theoretical surface roughness =  $(f/2)^2 / 2r$

$f$  = feed rate along contour =  $fx / \sin \phi$

$fx$  = feed rate in X axis

$r$  = tool edge radius

So in terms of X feed rate:

$$h = \left( \frac{fx}{2 \sin \phi} \right)^2 \frac{1}{2r}$$

For a known tool radius and a desired surface roughness (PTV cusp height) the feed rate in X axis is calculated by:

$$fx = (2\sqrt{2hr}) \sin \phi$$

Figure 12. Feed Rate Effects on Surface Finish

UNCLASSIFIED

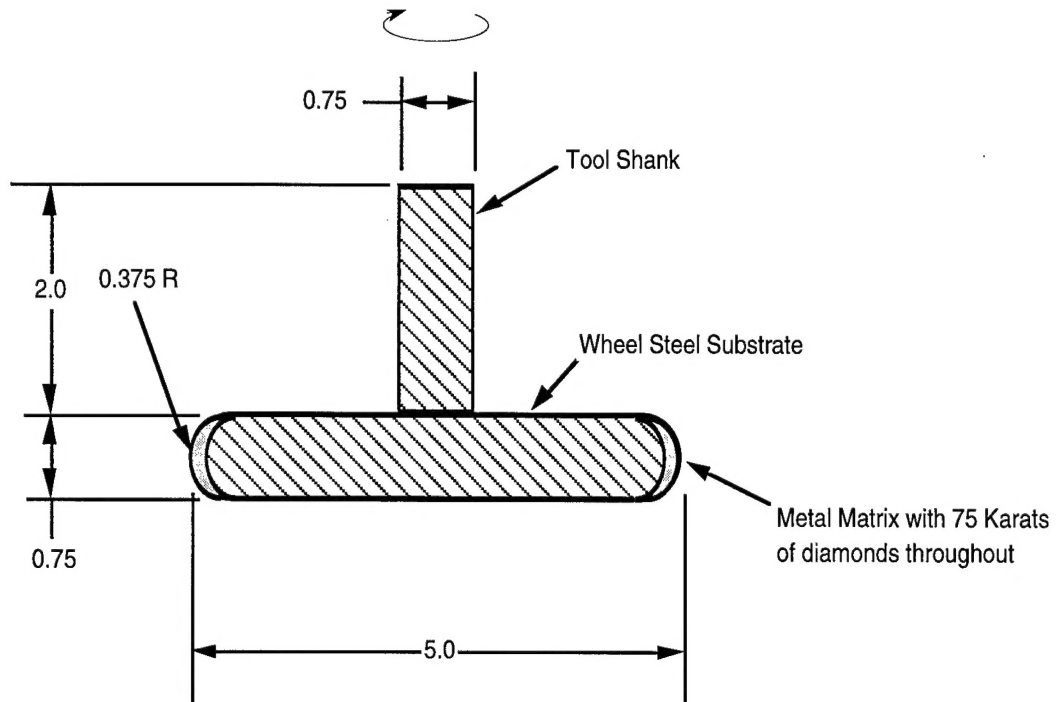


Figure 13. Diamond Grinding Wheel Sketch

UNCLASSIFIED